A PHASE-FIELD MODEL AND ITS NUMERICAL APPROXIMATION FOR TWO-PHASE INCOMPRESSIBLE FLOWS WITH DIFFERENT DENSITIES AND VISCOSITIES*

JIE SHEN† AND XIAOFENG YANG‡

Abstract. Modeling and numerical approximation of two-phase incompressible flows with different densities and viscosities are considered. A physically consistent phase-field model that admits an energy law is proposed, and several energy stable, efficient, and accurate time discretization schemes for the coupled nonlinear phase-field model are constructed and analyzed. Ample numerical experiments are carried out to validate the correctness of these schemes and their accuracy for problems with large density and viscosity ratios.

1. Introduction. The interfacial dynamics about immiscible two-phase fluids have attracted much attention for more than a century. In recent years, the diffuse interface approach, whose origin can be traced back to [21] and [27], has been successfully used to model two-phase incompressible fluids under various situations (cf. [10, 1, 15, 11, 13, 29] and the references therein). In particular, the energetic variational phase-field approach leads to a well-posed nonlinear coupled system that satisfies an energy law, making it possible to design numerical schemes which satisfy a corresponding discrete energy law that automatically ensures their numerical stability (cf., for instance, [6, 12, 2]).

However, most of the analysis and simulation of the phase-field model for two-phase flows have been restricted to the matched density case or with a Boussinesq approximation. The main difficulty for two-phase flows with different density is that the standard phase-field model with variable density does not admit an energy law, making it difficult to carry out mathematical and numerical analysis. For problems with small density ratio, a common practice is to use a Boussinesq approximation where the variable density ρ is replaced by a background constant density ρ_0 while an external gravitational force is added to model the effect of density difference (cf., for instance, [13]). While using the Boussinesq approximation leads to a well-posed dissipative phase-field system, its physical validity is based on the assumption that the density ratio between the two phases is small. Hence, it cannot be used for two-phase flows with large density ratios. Thus, the first objective of this paper is to derive a phase-field model, for two-phase incompressible flows with variable density without assuming a small density ratio, that admits an energy law.

The second objective is to design efficient and accurate numerical schemes for this new model which consists of a coupled nonlinear system for the velocity, pressure, and

phase functions. How to design effective, energy stable numerical schemes for this nonlinear system is a challenging task. We shall combine several approaches which have proved efficient for the phase equations and for the Navier–Stokes equations, respectively, namely, the stabilized schemes (cf. [28]) for the phase equations and projection-type schemes [3, 26] for the Navier–Stokes equations. We shall construct several efficient time discretization schemes which satisfy a discrete energy law and which lead to, at each time step, a *weakly coupled* system for the velocity and phase function and an elliptic equation for the pressure. Note that the elliptic equation for the pressure resultant from a projection-type scheme involves the density as a variable coefficient. In the case of a large density ratio, solving this elliptic equation for pressure usually takes most of the CPU time (sometimes more than 90% of the total cost). Therefore, we shall propose a pressure-stabilized formulation which only requires solving a Poisson equation for the pressure.

The third objective is to validate the new model and the proposed numerical schemes through careful numerical simulations, including the dynamics of an air bubble rising in water, a particularly challenging situation where the density ratio is close to 1000 and the viscosity ratio is close to 70.

The rest of the paper is organized as follows. In the next section, we derive a new phase-field model for two-phase incompressible flows with different densities and viscosities that admits an energy law. Then, in section 3, we describe in detail several efficient time discretization schemes and establish discrete energy laws which are in the same spirit of the continuous discrete energy law. In section 4, we present several numerical results to illustrate the effectiveness and the correctness of these numerical schemes. We conclude with a few remarks in the last section.

2. A new phase-field model for two-phase flows with variable density and viscosity. We consider a mixture of two immiscible, incompressible fluids with densities ρ_1, ρ_2 and viscosities μ_1, μ_2. In order to identify the regions occupied by the two fluids, we introduce a phase function ϕ such that

$$(2.1) \qquad \phi(x,t) = \begin{cases} 1 & \text{fluid 1,} \\ -1 & \text{fluid 2,} \end{cases}$$

with a thin smooth transition layer of thickness η connecting the two fluids so the interface of the mixture can be described by $\Gamma_t = \{x : \phi(x,t) = 0\}$. Let $F(\phi) = \frac{1}{4\eta^2}(\phi^2 - 1)^2$ be the Ginzburg–Landau double-well potential, and define the mixing energy functional

$$(2.2) \qquad W(\phi, \nabla\phi) = \int_\Omega \left(\frac{1}{2}|\nabla\phi|^2 + F(\phi) \right) dx,$$

which represents the competition between the hydrophilic and hydrophobic properties of the two-phase flow. We can then determine the dynamics of the phase function ϕ by a gradient flow

$$(2.3) \qquad \phi_t + (u \cdot \nabla)\phi = -\gamma \frac{\delta W}{\delta \phi},$$

where the variational derivative $\frac{\delta W}{\delta \phi}$ can be taken in H^{-1}, leading to the (conserved) Cahn–Hilliard phase equation

$$(2.4) \qquad \phi_t + (u \cdot \nabla)\phi = -\gamma \Delta(\Delta\phi - f(\phi)),$$

where $f(\phi) = F'(\phi)$, or in L^2, leading to the (nonconserved) Allen–Cahn phase equation

$$(2.5) \qquad \phi_t + (u \cdot \nabla)\phi = \gamma(\Delta\phi - f(\phi)).$$

For immiscible two-phase flows, we can introduce a nonlocal Lagrange multiplier $\xi(t)$ in the Allen–Cahn case to enforce the volume fraction conservation (cf. [28]), namely,

$$
\begin{aligned}
(2.6) \qquad & \phi_t + (u \cdot \nabla)\phi = \gamma(\Delta\phi - f(\phi) + \xi(t)), \\
& \frac{d}{dt}\int_\Omega \phi\, dx = 0.
\end{aligned}
$$

On the other hand, the momentum equation for the two-phase system takes the usual form

$$(2.7) \qquad \rho(u_t + (u \cdot \nabla)u) = \nabla \cdot \tau,$$

where the total stress $\tau = \mu D(u) - pI + \tau_e$ with $D(u) = \nabla u + \nabla u^T$ and τ_e is the extra elastic stress induced by the interfacial surface tension. It can be shown, using the least-action principle and the mixing energy functional defined above, that the momentum equation becomes

$$(2.8) \qquad \rho(u_t + (u \cdot \nabla)u) = \nabla \cdot (\mu D(u) - pI - \lambda(\nabla\phi \otimes \nabla\phi)),$$

where λ is the mixing energy density.

In the above, ρ and μ are slave variables defined by the linear average

$$(2.9) \qquad \rho(\phi) = \frac{\rho_1 - \rho_2}{2}\phi + \frac{\rho_1 + \rho_2}{2}, \; \mu(\phi) = \frac{\mu_1 - \mu_2}{2}\phi + \frac{\mu_1 + \mu_2}{2}.$$

Hence, the Cahn–Hilliard phase equation (2.4) (respectively, Allen–Cahn phase equation (2.6)) and the momentum equation (2.8), together with the incompressibility constraint

$$(2.10) \qquad \nabla \cdot u = 0$$

and suitable boundary and initial conditions, form a complete system for (u, p, ϕ) (respectively, (u, p, ϕ, ξ)) with ρ and μ given by (2.9).

When the density ratio is small, a usual approach is to use the Boussinesq approximation, i.e., replacing (2.8) by

$$(2.11) \qquad \rho_0(u_t + (u \cdot \nabla)u) = \nabla \cdot (\mu D(u) - pI - \lambda(\nabla\phi \otimes \nabla\phi)) + g(\rho_1, \rho_2),$$

where $\rho_0 = \frac{\rho_1 + \rho_2}{2}$ and $g(\rho_1, \rho_2)$ is an additional gravitational force to account for the density difference. Taking the inner product of (2.11) with u and that of (2.4) with $-\lambda(\Delta\phi - f(\phi))$, with suitable boundary conditions for u and ϕ, and using the identity

$$(2.12) \qquad \nabla \cdot (\nabla\phi \otimes \nabla\phi) = \Delta\phi\nabla\phi + \frac{1}{2}\nabla|\nabla\phi|^2,$$

we find that the Cahn–Hilliard phase-field system (2.4)-(2.10)-(2.11) admits the following energy law:

$$
\begin{aligned}
(2.13) \qquad & \frac{d}{dt}\int_\Omega \left(\frac{1}{2}\rho_0|u|^2 + \frac{\lambda}{2}|\nabla\phi|^2 + \lambda F(\phi)\right) dx \\
& = \int_\Omega g\, u\, dx - \int_\Omega \left(\frac{\mu}{2}|D(u)|^2 + \lambda\gamma|\nabla(\Delta\phi - f(\phi))|^2\right) dx.
\end{aligned}
$$

Similarly, for the Allen–Cahn phase-field system (2.6)-(2.10)-(2.11), we have

$$
(2.14) \quad
\begin{aligned}
&\frac{d}{dt} \int_\Omega \left(\frac{1}{2}\rho_0 |u|^2 + \frac{\lambda}{2}|\nabla\phi|^2 + \lambda F(\phi) \right) dx \\
&= \int_\Omega g\, u\, dx - \int_\Omega \left(\frac{\mu}{2}|D(u)|^2 + \lambda\gamma |\Delta\phi - f(\phi) + \xi(t)|^2 \right) dx.
\end{aligned}
$$

Unfortunately, to the best of the authors' knowledge, there is no corresponding energy law available for the original system (2.4)-(2.8)-(2.10) or (2.6)-(2.8)-(2.10). Therefore, our first task is to modify the above system in a physically consistent way to obtain a system which admits an energy law.

A critical property of the nonlinear term for the Navier–Stokes equations (with constant density) is the skew-symmetric property

$$
(2.15) \quad \int_\Omega \rho_0 (u \cdot \nabla)v \cdot v\, dx = 0 \text{ if } \nabla \cdot u = 0,\ u \cdot v|_\Gamma = 0, \text{ and } v \text{ is sufficiently smooth,}
$$

which does not hold if the constant ρ_0 in the above is replaced by a nonconstant function ρ. To overcome this difficulty, Guermond and Quartapelle [7] introduced a new variable $\sigma = \sqrt{\rho}$ in place of ρ. Using the mass conservation

$$
(2.16) \quad \rho_t + \nabla \cdot (\rho u) = 0,
$$

one derives

$$
(2.17) \quad \sigma(\sigma u)_t = \rho u_t + \frac{1}{2}\rho_t u = \rho u_t - \frac{1}{2}\nabla \cdot (\rho u)u.
$$

Therefore, it is physically consistent to replace ρu_t in (2.8) by $\sigma(\sigma u)_t + \frac{1}{2}\nabla \cdot (\rho u)u$, leading to the modified momentum equation

$$
(2.18) \quad \sigma(\sigma u)_t + (\rho u \cdot \nabla)u + \frac{1}{2}\nabla \cdot (\rho u)u - \nabla \cdot \mu D(u) + \nabla p + \lambda\nabla \cdot (\nabla\phi \otimes \nabla\phi) = 0.
$$

The main advantage of the new formulation is that the following desired property holds:

$$
(2.19) \quad \int_\Omega (\rho u \cdot \nabla)v \cdot v\, dx + \frac{1}{2}\int_\Omega \nabla \cdot (\rho u)v \cdot v\, dx = 0 \text{ if } u \cdot n|_\Gamma = 0.
$$

With the above identity, a similar procedure as before shows that the modified Cahn–Hilliard phase-field system (2.4)-(2.10)-(2.18) admits the following energy law:

$$
(2.20) \quad
\begin{aligned}
&\frac{d}{dt} \int_\Omega \left(\frac{1}{2}|\sigma u|^2 + \frac{\lambda}{2}|\nabla\phi|^2 + \lambda F(\phi) \right) dx \\
&= - \int_\Omega \left(\frac{\mu}{2}|D(u)|^2 + \lambda\gamma |\nabla(\Delta\phi - f(\phi))|^2 \right) dx.
\end{aligned}
$$

Similarly, for the modified Allen–Cahn phase-field system (2.6)-(2.10)-(2.18), we have

$$
(2.21) \quad
\begin{aligned}
&\frac{d}{dt} \int_\Omega \left(\frac{1}{2}|\sigma u|^2 + \frac{\lambda}{2}|\nabla\phi|^2 + \lambda F(\phi) \right) dx \\
&= - \int_\Omega \left(\frac{\mu}{2}|D(u)|^2 + \lambda\gamma |\Delta\phi - f(\phi) + \xi(t)|^2 \right) dx.
\end{aligned}
$$

3. Time discretizations and their stability analysis. In this section, we study time discretizations of the new phase-field model introduced in the last section. The goal is to construct time discretization schemes which satisfy a discrete energy law similar to the continuous case (2.21) and are easy to solve in practice.

To fix the idea and simplify the presentation, we shall consider only the Allen–Cahn phase-field system (2.5)-(2.10)-(2.18). We omit the Lagrange multiplier $\xi(t)$ in (2.6) as it does not introduce any computational or analytical difficulties. The time discretization of the Cahn–Hilliard phase-field system (2.4)-(2.10)-(2.18) can be treated in essentially the same fashion, except that its full discretization is more challenging due to the fourth-order spatial derivatives.

Let us first reformulate the system (2.5)-(2.10)-(2.18) into an equivalent form which is more convenient for numerical approximation.

Thanks to the maximum principle for the Allen–Cahn phase equation (2.6), we can truncate the double-well potential $F(\phi)$ to quadratic growth for $|\phi| > 1$ without affecting the solution. More precisely, we replace $F(\phi)$ by

$$
(3.1) \qquad F(\phi) = \begin{cases} \frac{1}{\eta^2}(\phi - 1)^2, & \phi > 1, \\ \frac{1}{4\eta^2}(\phi^2 - 1)^2, & \phi \in [-1, 1], \\ \frac{1}{\eta^2}(\phi + 1)^2, & \phi < -1. \end{cases}
$$

Then setting $f(\phi) = F'(\phi)$, we have

$$
(3.2) \qquad \max_{\phi \in \mathbb{R}} |f'(\phi)| \le \frac{2}{\eta^2}.
$$

On the other hand, using the identity (2.12), the phase equation (2.6), and the fact that $f(\phi)\nabla\phi = \nabla F(\phi)$, we have

$$
(3.3) \quad \nabla p + \lambda \nabla \cdot (\nabla\phi \otimes \nabla\phi) = \nabla\left(p + \frac{1}{2}\lambda|\nabla\phi|^2 + \lambda F(\phi)\right) + \frac{\lambda}{\gamma}(\phi_t + u \cdot \nabla\phi)\nabla\phi.
$$

Therefore, if we define the modified pressure as $\tilde{p} = p + \frac{1}{2}\lambda|\nabla\phi|^2 + \lambda F(\phi)$ and still denote it by p for simplicity, we can rewrite the system (2.5)-(2.10)-(2.18) as

(3.4a) $\phi_t + u \cdot \nabla\phi = \gamma(\Delta\phi - f(\phi))$,

(3.4b) $\rho(\phi) = \dfrac{\rho_1 - \rho_2}{2}\phi + \dfrac{\rho_1 + \rho_2}{2}, \quad \mu(\phi) = \dfrac{\mu_1 - \mu_2}{2}\phi + \dfrac{\mu_1 + \mu_2}{2}$,

(3.4c) $\sigma(\sigma u)_t + (\rho u \cdot \nabla)u + \dfrac{1}{2}\nabla \cdot (\rho u)u - \nabla \cdot \mu D(u) + \nabla p + \dfrac{\lambda}{\gamma}(\phi_t + u \cdot \nabla\phi)\nabla\phi = 0$,

(3.4d) $\nabla \cdot u = 0$.

To fix the idea, we consider the boundary conditions

$$
(3.5) \qquad u|_{\partial\Omega} = 0, \quad \frac{\partial\phi}{\partial n}\Big|_{\partial\Omega} = 0.
$$

We note that a similar reformulation is considered in [12] for a liquid crystal flow.

Taking the inner product of (3.4a) with $\frac{\lambda}{\gamma}(\phi_t + u \cdot \nabla\phi)$ and that of (3.4c) with u, we find

$$
(3.6) \qquad \begin{aligned} &\frac{d}{dt}\int_\Omega \left(\frac{1}{2}|\sigma u|^2 + \frac{\lambda}{2}|\nabla\phi|^2 + \lambda F(\phi)\right) dx \\ &\qquad = -\int_\Omega \left(\frac{\mu}{2}|D(u)|^2 + \frac{\lambda}{\gamma}|\phi_t + u \cdot \nabla\phi|^2\right) dx. \end{aligned}
$$

The above coupled nonlinear system presents formidable challenges for algorithm design, analysis, and implementation, particularly so when the density ratio is large. In this section, we shall design numerical algorithms which admit an energy law and overcome three main difficulties associated with this coupled nonlinear system, namely, (i) the coupling of the velocity and pressure with variable density and viscosity, (ii) the stiffness associated with the interfacial width η, and (iii) the pressure solver with a large density ratio.

- A common strategy to decouple the computation of the pressure from the velocity is to use a projection-type scheme as in the case for Navier–Stokes equations (cf., for instance, a recent review in [9]). However, most of the numerical analysis for projection-type schemes are limited to problems with constant density and viscosity. The few exceptions which deal with variable density are [7, 19, 8], which serve as inspiration for the numerical schemes we present below. We note that in [14], the authors considered a mixed finite element scheme for the Navier–Stokes equations with variable density and with the viscosity as a given function of the density.
- To alleviate the difficulty associated with the stiffness caused by the thin interfacial width, we introduce a stabilizing term in the phase equation as in [28, 22]. This stabilizing term allows us to treat the nonlinear term in the phase equation explicitly without suffering from any time step constraint.
- A typical projection type scheme will lead to an elliptic equation with density as a variable coefficient for the pressure. The numerical solution of this elliptic equation could become very expensive when the density ratio is large. We shall consider a pressure stabilized formulation to avoid solving a pressure elliptic equation with density as a variable coefficient.

Finally, we need to combine these ideas together to construct efficient and energy stable schemes for the coupled nonlinear system (3.4).

3.1. A scheme based on the Chorin–Temam projection method. For the sake of clarity, we shall first present a simple scheme based on the Chorin–Temam projection method. While this scheme lacks sufficient accuracy and is not recommended in practice, it embodies most of the essential ideas in the more accurate schemes that we construct subsequently.

Since the solution of a discretized phase equation does not necessarily satisfy a maximum principle, we set

$$(3.7) \qquad \hat{\phi} = \begin{cases} \phi, & |\phi| \leq 1, \\ \mathrm{sign}(\phi), & |\phi| > 1, \end{cases}$$

and we shall use it to update the density and viscosity so as to keep their positivity.

Our first scheme reads as follows:

Given initial conditions u^0 and ϕ^0, we compute $(\phi^{n+1}, \tilde{u}^{n+1}, u^{n+1}, p^{n+1})$ for $n \geq 0$ by

$$(3.8a) \quad \begin{cases} \dfrac{1}{\delta t}(\phi^{n+1} - \phi^n) + (\tilde{u}^{n+1} \cdot \nabla)\phi^n + \dfrac{\gamma}{\eta^2}(\phi^{n+1} - \phi^n) - \gamma(\Delta\phi^{n+1} - f(\phi^n)) = 0, \\ \partial_n \phi^{n+1}|_{\partial\Omega} = 0; \end{cases}$$

(3.8b)
$$\rho^{n+1} = \frac{\rho_1 - \rho_2}{2}\hat{\phi}^{n+1} + \frac{\rho_1 + \rho_2}{2}, \quad \mu^{n+1} = \frac{\mu_1 - \mu_2}{2}\hat{\phi}^{n+1} + \frac{\mu_1 + \mu_2}{2}, \quad \sigma^{n+1} = \sqrt{\rho^{n+1}};$$

$$(3.8c) \begin{cases} \sigma^{n+1}\dfrac{\sigma^{n+1}\tilde{u}^{n+1}-\sigma^n u^n}{\delta t} + \rho^n(u^n\cdot\nabla)\tilde{u}^{n+1} + \dfrac{1}{2}(\nabla\cdot(\rho^n u^n))\tilde{u}^{n+1} \\[2mm] \qquad -\nabla\cdot\mu^{n+1}D(\tilde{u}^{n+1}) + \dfrac{\lambda}{\gamma}\left(\dfrac{1}{\delta t}(\phi^{n+1}-\phi^n)+(\tilde{u}^{n+1}\cdot\nabla)\phi^n\right)\nabla\phi^n = 0, \\[2mm] \tilde{u}^{n+1}|_{\partial\Omega}=0; \end{cases}$$

$$(3.8d) \begin{cases} \rho^{n+1}\dfrac{u^{n+1}-\tilde{u}^{n+1}}{\delta t}+\nabla p^{n+1}=0, \\[2mm] \nabla\cdot u^{n+1}=0, \\[2mm] n\cdot u^{n+1}|_{\partial\Omega}=0. \end{cases}$$

Several remarks are in order.

Remark 3.1. A stabilizing term $\frac{\gamma}{\eta^2}(\phi^{n+1}-\phi^n)$ is introduced in (3.8a). This term introduces an additional consistency error of order $\frac{\gamma\delta t}{\eta^2}\phi'(\xi)$ which is of the same order as the error introduced by the explicit treatment of $f(\phi)$.

From (3.7) and (3.8b), we have $\rho_1 \le \rho^{n+1} \le \rho_2$ and $\mu_1 \le \mu^{n+1} \le \mu_2$, so σ^{n+1} is well defined.

The equations (3.8a) through (3.8c) form a *weakly coupled* system, for if we replace $\tilde{u}^{n+1}$ by $\tilde{u}^n$ in (3.8a), then we can obtain ϕ^{n+1} and $\tilde{u}^{n+1}$ by solving two decoupled *linear* elliptic equations. The system is only *weakly nonlinear* through σ^{n+1} in (3.8c). Thus, it can be efficiently solved by either decoupling the *weakly coupled* system with a lagged velocity for the convective term in the phase equation or using a simple subiteration process.

Equation (3.8d) is decoupled from the other equations. An equivalent formulation is

$$(3.9) \qquad \left(\frac{1}{\rho^{n+1}}\nabla p^{n+1},\nabla q\right) = \frac{1}{\delta t}(\tilde{u}^{n+1},\nabla q) \quad \text{for all } q\in H^1(\Omega),$$
$$u^{n+1}=\tilde{u}^{n+1}-\delta t\frac{1}{\rho^{n+1}}\nabla p^{n+1}.$$

Thus, an elliptic equation with variable $\frac{1}{\rho^{n+1}}$ needs to be solved at each time step.

We show below that the above scheme admits a discrete energy law. To simplify the notation, we denote

$$(3.10) \qquad \dot{\phi}^{n+1}=\frac{1}{\delta t}(\phi^{n+1}-\phi^n)+(\tilde{u}^{n+1}\cdot\nabla)\phi^n.$$

THEOREM 3.1. *The solution of scheme* (3.8) *satisfies the following discrete energy law:*

$$\|\sigma^{n+1}u^{n+1}\|_{L^2}^2 + \lambda\|\nabla\phi^{n+1}\|_{L^2}^2 + 2\lambda(F(\phi^{n+1}),1)$$
$$+ \delta t\left(\frac{2\lambda}{\gamma}\|\dot{\phi}^{n+1}\|_{L^2}^2 + \|\sqrt{\mu^{n+1}}D(\tilde{u}^{n+1})\|_{L^2}^2\right)$$
$$\le \|\sigma^n u^n\|_{L^2}^2 + \lambda\|\nabla\phi^n\|_{L^2}^2 + 2\lambda(F(\phi^n),1).$$

Proof. Taking the inner product of (3.8c) with $2\delta t\tilde{u}^{n+1}$ and using (2.19) and

$$(3.11) \qquad 2\delta t(\mu^{n+1}D(\tilde{u}^{n+1}),\nabla\tilde{u}^{n+1}) = \delta t\|\sqrt{\mu^{n+1}}D(\tilde{u}^{n+1})\|_{L^2}^2,$$

we derive

$$
(3.12) \quad
\begin{aligned}
&\|\sigma^{n+1}\tilde{u}^{n+1}\|_{L^2}^2 - \|\sigma^n u^n\|_{L^2}^2 + \|\sigma^{n+1}\tilde{u}^{n+1} - \sigma^n u^n\|_{L^2}^2 \\
&\qquad + \delta t \|\sqrt{\mu^{n+1}}D(\tilde{u}^{n+1})\|_{L^2}^2 + \frac{2\lambda\delta t}{\gamma}(\dot{\phi}^{n+1}\nabla\phi^n, \tilde{u}^{n+1}) = 0.
\end{aligned}
$$

Taking the inner product of (3.8d) with $2\delta t u^{n+1}$, we obtain

$$
(3.13) \quad \|\sigma^{n+1}u^{n+1}\|_{L^2}^2 + \|\sigma^{n+1}(u^{n+1} - \tilde{u}^{n+1})\|_{L^2}^2 = \|\sigma^{n+1}\tilde{u}^{n+1}\|_{L^2}^2.
$$

Combining the above inequalities and using (3.2), we find

$$
(3.14) \quad
\begin{aligned}
&\|\sigma^{n+1}u^{n+1}\|_{L^2}^2 - \|\sigma^n u^n\|_{L^2}^2 + \|\sigma^{n+1}(u^{n+1} - \tilde{u}^{n+1})\|_{L^2}^2 + \|\sigma^{n+1}\tilde{u}^{n+1} - \sigma^n u^n\|_{L^2}^2 \\
&\qquad + \delta t \|\sqrt{\mu^{n+1}}D(\tilde{u}^{n+1})\|_{L^2}^2 + \frac{2\lambda\delta t}{\gamma}(\dot{\phi}^{n+1}\nabla\phi^n, \tilde{u}^{n+1}) = 0.
\end{aligned}
$$

Taking the inner product of (3.8a) with $\frac{2\lambda}{\gamma}(\phi^{n+1} - \phi^n)$, we have

$$
(3.15) \quad
\begin{aligned}
&\frac{2\lambda\delta t}{\gamma}\|\dot{\phi}^{n+1}\|_{L^2}^2 - \frac{2\lambda\delta t}{\gamma}(\dot{\phi}^{n+1}, \tilde{u}^{n+1}\cdot\nabla\phi^n) + \frac{2\lambda}{\eta^2}\|\phi^{n+1} - \phi^n\|_{L^2}^2 \\
&\qquad + \lambda(\|\nabla\phi^{n+1}\|_{L^2}^2 - \|\nabla\phi^n\|_{L^2}^2 + \|\nabla\phi^{n+1} - \nabla\phi^n\|_{L^2}^2) \\
&\qquad + 2\lambda(f(\phi^n), \phi^{n+1} - \phi^n) = 0.
\end{aligned}
$$

For the last term in (3.15), we use the Taylor expansion

$$
(3.16) \quad F(\phi^{n+1}) - F(\phi^n) = f(\phi^n)(\phi^{n+1} - \phi^n) + \frac{f'(\xi^n)}{2}(\phi^{n+1} - \phi^n)^2.
$$

Combining (3.14), (3.15), and (3.16), we obtain

$$
\begin{aligned}
&\|\sigma^{n+1}u^{n+1}\|_{L^2}^2 - \|\sigma^n u^n\|_{L^2}^2 + \delta t\|\sqrt{\mu^{n+1}}D(\tilde{u}^{n+1})\|_{L^2}^2 + \frac{2\lambda\delta t}{\gamma}\|\dot{\phi}^{n+1}\|_{L^2}^2 \\
&\qquad + \frac{2\lambda}{\eta^2}\|\phi^{n+1} - \phi^n\|_{L^2}^2 + \lambda(\|\nabla\phi^{n+1}\|_{L^2}^2 - \|\nabla\phi^n\|_{L^2}^2 + \|\nabla\phi^{n+1} - \nabla\phi^n\|_{L^2}^2) \\
&\qquad + 2\lambda(F(\phi^{n+1}) - F(\phi^n), 1) \\
&\qquad \le \lambda(f'(\xi^n)(\phi^{n+1} - \phi^n), \phi^{n+1} - \phi^n) \le \frac{2\lambda}{\eta^2}\|\phi^{n+1} - \phi^n\|_{L^2}^2.
\end{aligned}
$$

Then, the desired result follows from the above inequality. $\square$

It is well known (cf., for instance, [23]) that the Chorin–Temam projection scheme is first-order accurate for the velocity in the L^2 norm and $\frac{1}{2}$-order accurate for the velocity in the H^1 norm and pressure in the L^2 norm. Furthermore, replacing the backward Euler discretization in (3.8) by a higher-order backward difference formula (BDF) will not improve the accuracy. Therefore, scheme (3.8) is not suitable in practice due to its poor accuracy. Below we shall construct more accurate numerical schemes with similar computational simplicity.

3.2. Schemes based on a gauge-Uzawa formulation. In [7], the authors proposed some projection-type schemes for the Navier–Stokes equations and proved their stability. However, their more accurate versions based on the pressure correction require two pressure solvers at each time step. In [19], the authors constructed two

schemes based on a gauge-Uzawa formulation [16] which is a modified version of the original gauge method [5]. The schemes in [19] require only one pressure solver at each time step, while having the same order of accuracy as the schemes in [7]. Following the approach in [19], we construct below a first-order gauge-Uzawa scheme for the phase-field model (3.4).

Given are initial conditions ϕ^0, $s^0 = 0$, and u^0 and set $\bar{\mu} = \min(\mu_1, \mu_2)$. We compute $(\phi^{n+1}, \tilde{u}^{n+1}, u^{n+1}, s^{n+1})$ for $n \geq 0$ by

(3.17a)
$$\begin{cases} \dfrac{1}{\delta t}(\phi^{n+1} - \phi^n) + (\tilde{u}^{n+1} \cdot \nabla)\phi^n + \dfrac{\gamma}{\eta^2}(\phi^{n+1} - \phi^n) - \gamma(\Delta\phi^{n+1} - f(\phi^n)) = 0, \\ \partial_n \phi^{n+1}|_{\partial\Omega} = 0; \end{cases}$$

(3.17b)
$$\rho^{n+1} = \frac{\rho_1 - \rho_2}{2}\hat{\phi}^{n+1} + \frac{\rho_1 + \rho_2}{2}, \quad \mu^{n+1} = \frac{\mu_1 - \mu_2}{2}\hat{\phi}^{n+1} + \frac{\mu_1 + \mu_2}{2}, \quad \sigma^{n+1} = \sqrt{\rho^{n+1}};$$

(3.17c)
$$\begin{cases} \sigma^{n+1}\dfrac{\sigma^{n+1}\tilde{u}^{n+1} - \sigma^n u^n}{\delta t} + \rho^n(u^n \cdot \nabla)\tilde{u}^{n+1} \\ \qquad\qquad\qquad + \dfrac{1}{2}(\nabla \cdot (\rho^n u^n))\tilde{u}^{n+1} - \nabla \cdot \mu^{n+1} D(\tilde{u}^{n+1}) \\ \qquad + \bar{\mu}\nabla s^n + \dfrac{\lambda}{\gamma}\left(\dfrac{1}{\delta t}(\phi^{n+1} - \phi^n) + (\tilde{u}^{n+1} \cdot \nabla)\phi^n\right)\nabla\phi^n = 0, \\ \tilde{u}^{n+1}|_{\partial\Omega} = 0; \end{cases}$$

(3.17d)
$$\begin{cases} -\nabla \cdot \left(\dfrac{1}{\rho^{n+1}}\nabla\psi^{n+1}\right) = \nabla \cdot \tilde{u}^{n+1}, \\ \partial_n \psi^{n+1} = 0; \end{cases}$$

(3.17e)
$$\begin{cases} u^{n+1} = \tilde{u}^{n+1} + \dfrac{1}{\rho^{n+1}}\nabla\psi^{n+1}, \\ s^{n+1} = s^n - \nabla \cdot \tilde{u}^{n+1}. \end{cases}$$

Remark 3.2. In the above, s^n is the so-called gauge variable. Although the pressure does not appear explicitly in the scheme, a proper approximation to the pressure is [19]

(3.18)
$$p^{n+1} = -\frac{\psi^{n+1}}{\delta t} + \bar{\mu}s^{n+1}.$$

Similar to (3.8), the above scheme involves a weakly coupled system for $(\phi^{n+1}, \tilde{u}^{n+1})$ and an elliptic equation with density as variable coefficient for the pseudopressure "ψ^{n+1}." When the density ratio is large, it becomes very difficult to solve this equation efficiently. This difficulty is shared by all projection-based schemes since they all involve projecting the nonsolenoidal provisional velocity onto the divergence-free space as in (3.17d) and (3.17e).

We have the following result for the scheme (3.17).

THEOREM 3.2. *The solution of scheme* (3.17) *satisfies the following discrete energy law:*

$$\|\sigma^k \tilde{u}^{n+1}\|_{L^2}^2 + \bar{\mu}\delta t\|s^{n+1}\|_{L^2}^2 + \lambda\|\nabla\phi^{n+1}\|_{L^2}^2 + 2\lambda(F(\phi^{n+1}), 1)$$
$$+ \delta t\left(\frac{2\lambda}{\gamma}\|\dot{\phi}^{n+1}\|_{L^2}^2 + \bar{\mu}\|\nabla\tilde{u}^{n+1}\|_{L^2}^2\right)$$
$$\leq \|\sigma^n \tilde{u}^n\|_{L^2}^2 + \bar{\mu}\delta t\|s^n\|_{L^2}^2 + \lambda\|\nabla\phi^n\|_{L^2}^2 + 2\lambda(F(\phi^n), 1).$$

Proof. Taking the inner product of (3.17b) with $2\delta t \tilde{u}^{n+1}$ and using (2.19) and (3.11), we obtain

$$\|\sigma^{n+1}\tilde{u}^{n+1}\|_{L^2}^2 - \|\sigma^n u^n\|_{L^2}^2 + \|\sigma^{n+1}\tilde{u}^{n+1} - \sigma^n u^n\|_{L^2}^2 + \delta t\|\sqrt{\mu^{n+1}}D(\tilde{u}^{n+1})\|_{L^2}^2$$

(3.19)
$$+ 2\bar{\mu}\delta t(\nabla s^n, \tilde{u}^{n+1}) + \frac{2\lambda\delta t}{\gamma}(\dot{\phi}^{n+1}\nabla\phi^n, \tilde{u}^{n+1}) = 0.$$

Using (3.17e), we obtain

$$(\sigma^n u^n, \sigma^n u^n) = (\rho^n u^n, u^n) = \left(\rho^n\left(\tilde{u}^n + \frac{1}{\rho^n}\nabla\psi^n\right), u^n\right) = (\rho^n\tilde{u}^n, u^n)$$

(3.20)
$$= \left(\rho^n\tilde{u}^n, \tilde{u}^n + \frac{1}{\rho^n}\nabla\psi^n\right) = \|\sigma^n\tilde{u}^n\|_{L^2}^2 + \left(u^n - \frac{1}{\rho^n}\nabla\psi^n, \nabla\psi^n\right)$$

$$= \|\sigma^n\tilde{u}^n\|_{L^2}^2 - \|\frac{1}{\sigma^n}\nabla\psi^n\|_{L^2}^2$$

and

$$2\bar{\mu}\delta t(\nabla s^n, \tilde{u}^{n+1}) = 2\bar{\mu}\delta t(s^n, -\nabla \cdot \tilde{u}^{n+1}) = 2\bar{\mu}\delta t(s^n, s^{n+1} - s^n)$$

(3.21)
$$= \bar{\mu}\delta t(\|s^{n+1}\|_{L^2}^2 - \|s^n\|_{L^2}^2 - \|s^{n+1} - s^n\|_{L^2}^2)$$

$$= \bar{\mu}\delta t(\|s^{n+1}\|_{L^2}^2 - \|s^n\|_{L^2}^2) - \bar{\mu}\delta t\|\nabla \cdot \tilde{u}^{n+1}\|_{L^2}^2.$$

It is easy to check by integration by parts that

(3.22)
$$\|D(u)\|_{L^2}^2 = \|\nabla u\|_{L^2}^2 + \|\nabla \cdot u\|_{L^2}^2 \quad \text{for all } u \in H_0^1(\Omega)^d.$$

Hence, we have

(3.23) $\bar{\mu}\|\nabla \cdot \tilde{u}^{n+1}\|_{L^2}^2 + \bar{\mu}\|\nabla\tilde{u}^{n+1}\|_{L^2}^2 = \|\sqrt{\bar{\mu}}D(\tilde{u}^{n+1})\|_{L^2}^2 \leq \|\sqrt{\mu^{n+1}}D(\tilde{u}^{n+1})\|_{L^2}^2.$

Combining the above inequalities, we find

$$\|\sigma^{n+1}\tilde{u}^{n+1}\|_{L^2}^2 - \|\sigma^n\tilde{u}^n\|_{L^2}^2 + \left\|\frac{1}{\sigma^n}\nabla\psi^n\right\|_{L^2}^2 + \|\sigma^{n+1}\tilde{u}^{n+1} - \sigma^n u^n\|_{L^2}^2$$

$$+ \bar{\mu}\delta t(\|s^{n+1}\|_{L^2}^2 - \|s^n\|_{L^2}^2) + \delta t\bar{\mu}\|\nabla\tilde{u}^{n+1}\|_{L^2}^2$$

$$+ \frac{2\lambda\delta t}{\gamma}(\dot{\phi}^{n+1}\nabla\phi^{n+1}, \tilde{u}^{n+1}) \leq 0.$$

Taking the inner product of (3.17a) with $\frac{2\lambda}{\gamma}(\phi^{n+1} - \phi^n)$ and using the same procedure as in the proof of Theorem 3.1, we can obtain

$$\|\sigma^{n+1}\tilde{u}^{n+1}\|_{L^2}^2 - \|\sigma^n\tilde{u}^n\|_{L^2}^2 + \left\|\frac{1}{\sigma^n}\nabla\psi^n\right\|_{L^2}^2 + \|\sigma^{n+1}\tilde{u}^{n+1} - \sigma^n u^n\|_{L^2}^2 + \delta t\bar{\mu}\|\nabla\tilde{u}^{n+1}\|_{L^2}^2$$

$$+ \bar{\mu}\delta t(\|s^{n+1}\|_{L^2}^2 - \|s^n\|_{L^2}^2) + \frac{2\lambda\delta t}{\gamma}\|\dot{\phi}^{n+1}\|_{L^2}^2$$

$$+ \lambda(\|\nabla\phi^{n+1}\|_{L^2}^2 - \|\nabla\phi^n\|_{L^2}^2 + \|\nabla\phi^{n+1} - \nabla\phi^n\|_{L^2}^2)$$

$$+ 2\lambda(F(\phi^{n+1}) - F(\phi^n), 1) \leq 0.$$

Then, the desired result follows from the above inequality.   ☐

It is clear that scheme (3.17) is only of first-order. However, a formally second-order scheme can be constructed by combining the second-order scheme in [19] and the approach for the phase equation in (3.17) as follows.

For the sake of simplicity, we shall denote, for any sequence $\{a^k\}$, $a^{*,k+1} = 2a^k - a^{k-1}$.

(3.24a)
$$
\begin{cases}
\dfrac{3\phi^{n+1} - 4\phi^n + \phi^{n-1}}{2\delta t} + (\tilde{u}^{n+1} \cdot \nabla)\phi^{*,n+1} \\
\qquad + \dfrac{\gamma}{\eta^2}(\phi^{n+1} - 2\phi^n + \phi^{n-1}) - \gamma(\Delta\phi^{n+1} - 2f(\phi^n) + f(\phi^{n-1})) = 0, \\
\partial_n\phi^{n+1}|_{\partial\Omega} = 0;
\end{cases}
$$

(3.24b) $\quad \rho^{n+1} = \dfrac{\rho_1 - \rho_2}{2}\hat{\phi}^{n+1} + \dfrac{\rho_1 + \rho_2}{2}, \ \mu^{n+1} = \dfrac{\mu_1 - \mu_2}{2}\hat{\phi}^{n+1} + \dfrac{\mu_1 + \mu_2}{2};$

(3.24c)
$$
\begin{cases}
\rho^{n+1}\dfrac{3\tilde{u}^{n+1} - 4u^n + u^{n-1}}{2\delta t} + \rho^{n+1}(u^{*,n+1} \cdot \nabla)\tilde{u}^{n+1} + \dfrac{1}{2}(\nabla \cdot (\rho^{n+1}u^{*,n+1}))\tilde{u}^{n+1} \\
\qquad - \nabla \cdot \mu^{n+1}D(\tilde{u}^{n+1}) + \nabla p^n + \bar{\mu}\nabla s^n \\
\qquad + \dfrac{\lambda}{\gamma}\left(\dfrac{1}{2\delta t}(3\phi^{n+1} - 4\phi^n + \phi^{n-1}) + (\tilde{u}^{n+1} \cdot \nabla)\phi^{*,n+1}\right)\nabla\phi^{*,n+1} = 0, \\
\tilde{u}^{n+1}|_{\partial\Omega} = 0;
\end{cases}
$$

(3.24d)
$$
\begin{cases}
-\nabla \cdot \left(\dfrac{1}{\rho^{n+1}}\nabla\psi^{n+1}\right) = \nabla \cdot \tilde{u}^{n+1}, \\
\partial_n\psi^{n+1} = 0;
\end{cases}
$$

(3.24e)
$$
\begin{cases}
u^{n+1} = \tilde{u}^{n+1} + \dfrac{1}{\rho^{n+1}}\nabla\psi^{n+1}, \\
s^{n+1} = s^n - \nabla \cdot \tilde{u}^{n+1}, \\
p^{n+1} = p^n - \dfrac{3}{2\delta t}\psi^{n+1} + \bar{\mu}s^{n+1}.
\end{cases}
$$

The numerical procedure for the second-order scheme (3.24) is exactly the same for the first-order scheme (3.17). However, while it appears possible to prove its stability, the process will be so technically complicated that we shall not pursue it in this paper.

3.3. Schemes based on pressure stabilization. As discussed in Remark 3.2, any scheme with a projection step would result in an elliptic equation with density as the variable coefficient. This observation led Guermond and Salgado [8] to construct a scheme for the Navier–Stokes equations with variable density, based on pressure stabilization (cf., for instance, [20, 25, 18, 9]), namely, the divergence-free condition is replaced by

(3.25)
$$
\nabla \cdot u - \delta\Delta p_t = 0,
$$

where δ is a small parameter.

Inspired by the incremental pressure stabilization scheme for the Navier–Stokes equations presented in [8], we propose the following first-order scheme.

Given are initial conditions ϕ^0, $p^0 = 0$, u^0, and set $\bar{\rho} = \min(\rho_1, \rho_2)$. We compute $(\phi^{n+1}, u^{n+1}, p^{n+1})$ for $n \geq 0$ by

(3.26a)
$$\begin{cases} \dfrac{\phi^{n+1} - \phi^n}{\delta t} + (u^{n+1} \cdot \nabla)\phi^n + \dfrac{\gamma}{\eta^2}(\phi^{n+1} - \phi^n) - \gamma(\Delta\phi^{n+1} - f(\phi^n)) = 0, \\ \partial_n \phi^{n+1}|_{\partial\Omega} = 0; \end{cases}$$

(3.26b)
$$\rho^{n+1} = \frac{\rho_1 - \rho_2}{2}\hat{\phi}^{n+1} + \frac{\rho_1 + \rho_2}{2}, \quad \mu^{n+1} = \frac{\mu_1 - \mu_2}{2}\hat{\phi}^{n+1} + \frac{\mu_1 + \mu_2}{2};$$

(3.26c)
$$\begin{cases} \dfrac{\frac{1}{2}(\rho^{n+1} + \rho^n)u^{n+1} - \rho^n u^n}{\delta t} + \rho^n(u^n \cdot \nabla)u^{n+1} \\ \qquad\qquad\qquad + \dfrac{1}{2}(\nabla \cdot (\rho^n u^n))u^{n+1} - \nabla \cdot \mu^{n+1} D(u^{n+1}) \\ \qquad + \nabla(2p^n - p^{n-1}) + \lambda\left(\dfrac{\phi^{n+1} - \phi^n}{\delta t} + (u^{n+1} \cdot \nabla)\phi^n\right)\nabla\phi^n = 0, \\ u^{n+1}|_{\partial\Omega} = 0; \end{cases}$$

(3.26d)
$$\begin{cases} \Delta(p^{n+1} - p^n) = \dfrac{\bar{\rho}}{\delta t}\nabla \cdot u^{n+1}, \\ \partial_n p^{n+1}|_{\partial\Omega} = 0. \end{cases}$$

The above scheme involves a weakly coupled system for (ϕ^{n+1}, u^{n+1}) and a Poisson equation for the pressure increment. So this scheme is computationally more efficient than (3.17), particularly when the density ratio is large. On the other hand, the above scheme does not lead to a divergence-free approximation while (3.17) does.

Let us denote

(3.27)
$$\dot{\phi}^{n+1} = \frac{\phi^{n+1} - \phi^n}{\delta t} + (u^{n+1} \cdot \nabla)\phi^n.$$

We have the following result.

THEOREM 3.3. *The solution of scheme* (3.26) *satisfies the following energy law:*

$$\|\sigma^{n+1}u^{n+1}\|_{L^2}^2 + \frac{\delta t^2}{\bar{\rho}}\|\nabla p^{n+1}\|_{L^2}^2 + \lambda\|\nabla\phi^{n+1}\|_{L^2}^2 + 2\lambda(F(\phi^{n+1}), 1)$$

$$+ \delta t\left(\frac{2\lambda}{\gamma}\|\dot{\phi}^{n+1}\|_{L^2}^2 + \|\mu^{n+1}D(u^{n+1})\|_{L^2}^2\right)$$

$$\leq \|\sigma^n u^n\|_{L^2}^2 + \frac{\delta t^2}{\bar{\rho}}\|\nabla p^n\|_{L^2}^2 + \lambda\|\nabla\phi^n\|_{L^2}^2 + 2\lambda(F(\phi^n), 1).$$

Proof. Taking the inner product of (3.26c) with $2\delta t u^{n+1}$ from

(3.28)
$$\left(\frac{1}{2}(\rho^{n+1} + \rho^n)u^{n+1} - \rho^n u^n, 2u^{n+1}\right) = \|\sigma^{n+1}u^{n+1}\|_{L^2}^2 - \|\sigma^n u^n\|_{L^2}^2$$
$$+ \|\sigma^n(u^{n+1} - u^n)\|_{L^2}^2$$

and using (2.19), we have

(3.29)
$$\|\sigma^{n+1}u^{n+1}\|_{L^2}^2 - \|\sigma^n u^n\|_{L^2}^2 + \|\sigma^n(u^{n+1} - u^n)\|_{L^2}^2 + \delta t\|\sqrt{\mu^{n+1}}D(u^{n+1})\|_{L^2}^2$$
$$+ 2\delta t(p^{n+1} - 2p^n + p^{n-1}, \nabla \cdot u^{n+1})$$
$$- 2\delta t(p^{n+1}, \nabla \cdot u^{n+1}) + \frac{2\lambda\delta t}{\gamma}(\dot{\phi}^{n+1}\nabla\phi^n, u^{n+1}) = 0.$$

Taking the inner product of (3.26d) with $\frac{2\delta t^2}{\bar{\rho}}(p^{n+1} - 2p^n + p^{n-1})$, we obtain

$$
\begin{aligned}
&-\frac{\delta t^2}{\bar{\rho}}(\|\nabla(p^{n+1} - p^n)\|_{L^2}^2 - \|\nabla(p^n - p^{n-1})\|_{L^2}^2 + \|\nabla(p^{n+1} - 2p^n + p^{n-1})\|_{L^2}^2) \\
&= 2\delta t(\nabla \cdot u^{n+1}, p^{n+1} - 2p^n + p^{n-1}).
\end{aligned}
$$
(3.30)

Taking the inner product of (3.26d) with $-\frac{2\delta t^2}{\bar{\rho}}p^{n+1}$, we obtain

$$
\begin{aligned}
&\frac{\delta t^2}{\bar{\rho}}(\|\nabla p^{n+1}\|_{L^2}^2 - \|\nabla p^n\|_{L^2}^2 + \|\nabla(p^{n+1} - p^n\|_{L^2}^2) \\
&= -2\delta t(\nabla \cdot u^{n+1}, p^{n+1}).
\end{aligned}
$$
(3.31)

After adding the above two equalities together, we have

$$
\begin{aligned}
&2\delta t(p^{n+1} - 2p^n + p^{n-1}, \nabla \cdot u^{n+1}) - 2\delta t(p^{n+1}, \nabla \cdot u^{n+1}) \\
&= \frac{\delta t^2}{\bar{\rho}}(\|\nabla p^{n+1}\|_{L^2}^2 - \|\nabla p^n\|_{L^2}^2) + \frac{\delta t^2}{\bar{\rho}}\|\nabla(p^n - p^{n-1})\|_{L^2}^2 \\
&\quad - \frac{\delta t^2}{\bar{\rho}}\|\nabla(p^{n+1} - 2p^n + p^{n-1})\|_{L^2}^2.
\end{aligned}
$$
(3.32)

Taking the difference of (3.26d) at step $n + 1$ and step n, we derive

$$
\frac{\delta t^2}{\bar{\rho}}\|\nabla(p^{n+1} - 2p^n + p^{n-1})\|_{L^2}^2 \leq \bar{\rho}\|u^{n+1} - u^n\|_{L^2}^2 \leq \|\sigma^n(u^{n+1} - u^n)\|_{L^2}^2.
$$
(3.33)

Combining the above inequalities together, we derive

$$
\begin{aligned}
&\|\sigma^{n+1}u^{n+1}\|_{L^2}^2 - \|\sigma^n u^n\|_{L^2}^2 + \delta t\|\sqrt{\mu^{n+1}}D(u^{n+1})\|_{L^2}^2 \\
&+ \frac{\delta t^2}{\bar{\rho}}(\|\nabla p^{n+1}\|_{L^2}^2 - \|\nabla p^n\|_{L^2}^2) + \frac{\delta t^2}{\bar{\rho}}\|\nabla(p^{n+1} - p^n)\|_{L^2}^2 \\
&+ \frac{2\lambda\delta t}{\gamma}(\dot{\phi}^{n+1}\nabla\phi^n, u^{n+1}) \leq 0.
\end{aligned}
$$
(3.34)

Taking the inner product of (3.26a) with $\frac{2\lambda}{\gamma}(\phi^{n+1} - \phi^n)$ and using the same procedure as in the proof of Theorem 3.1, finally we obtain

$$
\begin{aligned}
&\|\sigma^{n+1}u^{n+1}\|_{L^2}^2 - \|\sigma^n u^n\|_{L^2}^2 + \delta t\|\sqrt{\mu^{n+1}}D(u^{n+1})\|_{L^2}^2 \\
&\quad + \frac{\delta t^2}{\bar{\rho}}(\|\nabla p^{n+1}\|_{L^2}^2 - \|\nabla p^n\|_{L^2}^2) + \frac{\delta t^2}{\bar{\rho}}\|\nabla(p^{n+1} - p^n)\|_{L^2}^2 \\
&\quad + \frac{2\lambda\delta t}{\gamma}\|\dot{\phi}^{n+1}\|_{L^2}^2 + \lambda(\|\nabla\phi^{n+1}\|_{L^2}^2 - \|\nabla\phi^n\|_{L^2}^2 + \|\nabla\phi^{n+1} - \nabla\phi^n\|_{L^2}^2) \\
&\quad + 2\lambda(F(\phi^{n+1}) - F(\phi^n), 1) \leq 0. \quad \square
\end{aligned}
$$

We can construct a second-order version of scheme (3.26) by combining the approaches for the phase equation in (3.26) and for the velocity-pressure in [8]. As before, we still denote, for any sequence $\{a^k\}$, $a^{*,k+1} = 2a^k - a^{k-1}$. Then a second-order version of (3.26) reads

(3.35a)
$$\begin{cases} \frac{3\phi^{n+1} - 4\phi^n + \phi^{n-1}}{2\delta t} + (u^{n+1} \cdot \nabla)\phi^{*,n+1} + \frac{\gamma}{\eta^2}(\phi^{n+1} - 2\phi^n + \phi^{n-1}) \\ \qquad\qquad - \gamma(\Delta\phi^{n+1} - 2f(\phi^n) + f(\phi^{n-1})) = 0, \\ \partial_n\phi^{n+1}|_{\partial\Omega} = 0; \end{cases}$$

(3.35b)
$$\rho^{n+1} = \frac{\rho_1 - \rho_2}{2}\hat\phi^{n+1} + \frac{\rho_1 + \rho_2}{2}, \ \mu^{n+1} = \frac{\mu_1 - \mu_2}{2}\hat\phi^{n+1} + \frac{\mu_1 + \mu_2}{2};$$

(3.35c)
$$\begin{cases} \frac{\rho^{n+1}}{2\delta t}(3u^{n+1} - 4u^n + u^{n-1}) + \rho^{n+1}(\nabla \cdot u^{*,n+1})u^{n+1} \\ \qquad\qquad - \nabla \cdot \mu^{n+1}D(u^{n+1}) + \nabla\left(p^n + \frac{4}{3}\psi^n - \frac{1}{3}\psi^{n-1}\right) \\ \qquad + \frac{\lambda}{\gamma}\left(\frac{1}{2\delta t}(3\phi^{n+1} - 4\phi^n + \phi^{n-1}) + (u^{n+1} \cdot \nabla)\phi^{*,n+1}\right)\nabla\phi^{n+1} = 0, \\ u^{n+1}|_{\partial\Omega} = 0; \end{cases}$$

(3.35d)
$$\begin{cases} \Delta\psi^{n+1} = \frac{3\bar\rho}{2\delta t}\nabla \cdot u^{n+1}, \\ \partial_n\psi^{n+1}|_{\partial\Omega} = 0, \\ p^{n+1} = p^n + \psi^{n+1} - \mu^{n+1}\nabla \cdot u^{n+1}. \end{cases}$$

We note that the numerical procedure for the above scheme is exactly the same as that of scheme (3.26). However, while it is not hard to show that the above scheme is formally second-order accurate, it appears to be very difficult to extend the stability proof of scheme (3.26) to this second-order scheme.

4. Numerical results. In this section, we present some computational experiments using the numerical schemes constructed in the last section to demonstrate their efficiency and accuracy and the robustness of the phase-field model.

4.1. Brief description of the full discretization schemes. In all the following examples, we consider a two-dimensional rectangular domain. We adopt the spatial discretization based on the Legendre–Galerkin method [24] which results in very efficient and accurate solvers for elliptic equations with constant coefficients. We use the inf-sup stable (P_N, P_{N-2}) pair for the velocity and pressure (or the gauge or pseudopressure) and P_N for the phase function in all schemes.

The time discretization schemes constructed in the last section all lead to a *weakly coupled* system for the velocity and the phase function and an elliptic equation for the pressure. In order to take full advantage of the fast spectral Poisson solvers, we can either decouple the *weakly coupled* system using a lagged velocity for the convective term in the phase equation, which will lead to a time step constraint, or adopt a simple subiteration process, which requires solving a sequence of decoupled

elliptic equations at each time step to remove the time step constraint. Therefore, at each time step, all numerical schemes presented in the last section will reduce to a sequence of elliptic equations for the velocity u and phase function ϕ and an elliptic or Poisson equation (depending on which scheme to use) for the pressure p. The nonconstant coefficient elliptic problems will be solved by using a preconditioner conjugate gradient (PCG) method with a suitable constant-coefficient problem as a preconditioner [24]. This PCG approach is usually very effective for moderately varying coefficients. However, when the density ratio becomes large, the pressure equation in the gauge-Uzawa schemes (GUM) (3.17) and (3.24) could become very expensive. In this case, the pressure stabilization-based schemes (PSM) (3.26) and (3.35) become much more efficient than the GUM.

4.2. Accuracy test. In order to test the convergence rates, we consider the system (3.4) in $\Omega = (-1, 1)^2$ with $\mu = 1$ and suitable forcing functions such that the exact solution is given by

$$(4.1) \quad \begin{cases} \phi(t, x, y) = 2 + \sin(t)\cos(\pi x)\cos(\pi y), \\ \rho_1 = 3, \ \rho_2 = 1, \ \rho(t, x, y) = \phi(t, x, y) + 2 \\ u(t, x, y) = \pi \sin(2\pi y)\sin^2(\pi x)\sin(t), \\ v(t, x, y) = -\pi \sin(2\pi x)\sin^2(\pi y)\sin(t), \\ p(t, x, y) = \cos(\pi x)\sin(\pi y)\sin(t). \end{cases}$$
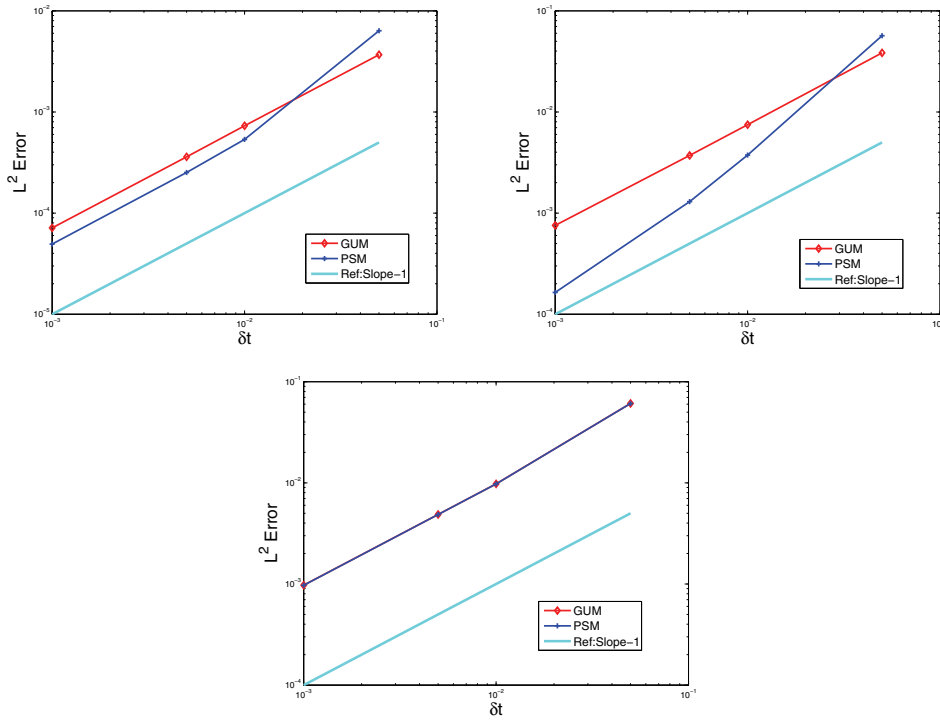
We used 129^2 Legendre–Gauss–Lobatto points so the spatial discretization errors are negligible compared with the time discretization error. In Figure 1, we plot the L^2 errors of the velocity, pressure, and density between the numerical solution and the exact solution at $t = 1$ with different time step sizes. It is clear from Figure 1(a) that the first-order GUM and PSM are first-order accurate in time for all variables and that the velocity and pressure approximations by PSM are slightly more accurate than those by GUM. On the other hand, we observe from Figure 1(b) that the second-order GUM and PSM appear to be second-order accurate for all variables except the pressure approximation by PSM, which appears to be first-order accurate; this is consistent with the pressure error estimate for the second-order PSM in [25]. It is also interesting to note that, contrary to the first-order case, the velocity and pressure approximations by the second-order GUM are more accurate than those by the second-order PSM.

4.3. A lighter bubble rising in a heavier medium. We now use system (3.4) to study a two-phase incompressible fluid in a rectangular domain $\Omega = (-d, d) \times (-2d, 2d)$ with initially a lighter bubble (with density ρ_1 and dynamic viscosity μ_1) in a heavier medium (with density ρ_2 and dynamic viscosity μ_2). The equations are nondimensionalized using the scaled variables
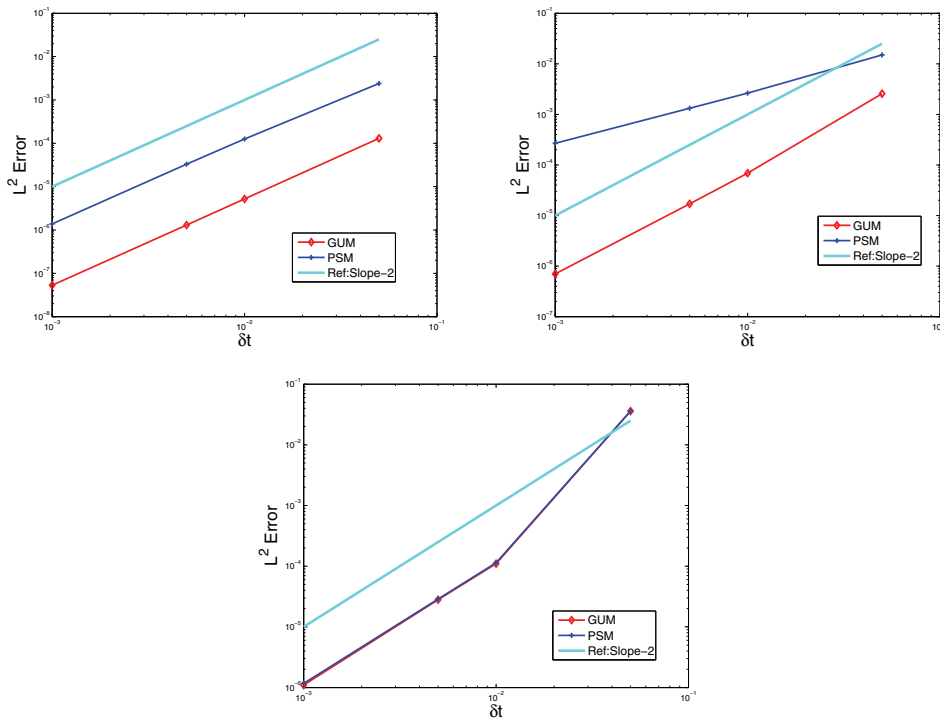
$$(4.2) \qquad \hat{t} = \frac{t}{t_0}, \quad \hat{\rho} = \frac{\rho}{\rho_0}, \quad \hat{x} = \frac{x}{d_0}, \quad \hat{u} = \frac{u}{u_0},$$

where

$$(4.3) \qquad t_0 = \sqrt{d/g}, \quad d_0 = \quad u_0 = \sqrt{dg}, \quad \rho_0 = \min(\rho_1, \rho_2).$$

(a) First-order PSM and GUM for velocity, pressure, and density, respectively.

(b) Second-order PSM and GUM for velocity, pressure, and density, respectively.

FIG. 1. *Convergence rate comparison of PSM and GUM.*

The dimensionless form of (3.4) with an extra gravitational force ρg in the momentum equation, after we omit the $\hat{\ }$ from the notation, is

$$(4.4) \qquad \phi_t + (u \cdot \nabla)\phi - \gamma \left(\Delta\phi - \frac{\phi(\phi^2 - 1)}{\eta^2} \right) = 0,$$

$$(4.5) \qquad \rho(\phi) = \frac{\tilde{\rho}_1 - \tilde{\rho}_2}{2}\phi + \frac{\tilde{\rho}_1 + \tilde{\rho}_2}{2}, \ \mu(\phi) = \frac{\tilde{\mu}_1 - \tilde{\mu}_2}{2}\phi + \frac{\tilde{\mu}_1 + \tilde{\mu}_2}{2},$$

$$(4.6) \qquad \sigma(\sigma u)_t + (\rho u \cdot \nabla)u + \frac{1}{2}\nabla \cdot (\rho u)u - \nabla \cdot (\mu\nabla u) + \nabla p + \frac{\lambda}{\gamma}\dot{\phi}\nabla\phi = 0,$$

$$(4.7) \qquad \nabla \cdot u = 0,$$

where $\tilde{\rho}_1 = \rho_1/\rho_0$, $\tilde{\rho}_2 = \rho_2/\rho_0$, $\tilde{\mu}_1 = \mu_1/(\rho_0 d^{3/2} g^{1/2})$, and $\tilde{\mu}_2 = \mu_2/(\rho_0 d^{3/2} g^{1/2})$. We set the initial velocity to be zero. The smoothed initial condition for ϕ is given by

$$(4.8) \qquad \phi(x, t = 0) = -\tanh\left(\frac{r - 0.5d}{\eta_0} \right),$$

where r is the distance from the center of the bubble to the point and η_0 is the diffusive interfacial width.

We emphasize that in order to conserve the volume fraction for the phase function, a Lagrange multiplier as in (2.6) is added in the above model and in the corresponding numerical schemes.

4.3.1. Low density ratio with homogeneous viscosity. We first examine the relative accuracy of different schemes in the last section for a problem with homogeneous viscosity and a low density ratio, $\rho_1 = 1$ and $\rho_2 = 10$. We set d = 0.005, g = 9.8, $\mu_1 = \mu_2 = 0.0011$, $\lambda = 0.001$, $\gamma = 0.02$, and $\eta_0 = \eta = 0.02d$. We use a grid size of 257^2 and a time step size of $\delta t = 0.001$. In Figure 2, we plot a detailed comparison of the level sets of $\{\phi : \phi = 0\}$ by first-order GUM and PSM at different times. No visual difference is observed, indicating that (i) the two schemes capture well the dynamics of the bubble evolution, and (ii) the new phase-field model is robust as the two very different numerical schemes produce identical results.

4.3.2. An air bubble rising in water. We now consider an air bubble rising in water. The physical parameters are $\rho_1 = 1.161$ and $\rho_2 = 995.65$ with $\mu_1 = 0.0000186$, and $\mu_2 = 0.0007977$. We set d = 0.005, g = 9.8, $\lambda = 0.001$, $\gamma = 0.02$, and $\eta_0 = \eta = 0.02d$. We use a grid size of 257^2 and a time step size of $\delta t = 0.0001$. In Figure 3, we plot a comparison of the level sets $\{\phi : \phi = 0\}$ by four different schemes at different times. We observe that the four different schemes, first- and second-order GUM and PSM, produce visually identical results, indicating that all four schemes can be used for challenging two-phase flow simulations. It is interesting to note that the results in Figure 3 appear to be very similar to those in Figure 18 in [17] which was computed by using an adaptive volume-of-fluid approach under a similar physical situation.

We note that while the parameters we used here correspond to the physical situation, the two-dimensional rectangular domain we used is not physical, so the numerical results cannot really be validated against the experiments. Since our main objective in this paper is to construct efficient numerical schemes that are energy stable and to show their effectiveness in practice, we shall defer the three-dimensional or two-dimensional axisymmetric simulations and their comparisons with recent results (cf. [4, 17]) to a future study.

To summarize, all four numerical schemes produce accurate and reasonable results as long as δt is sufficiently small, particularly in the case of high density ratios. These results are consistent with the analysis in the last section.
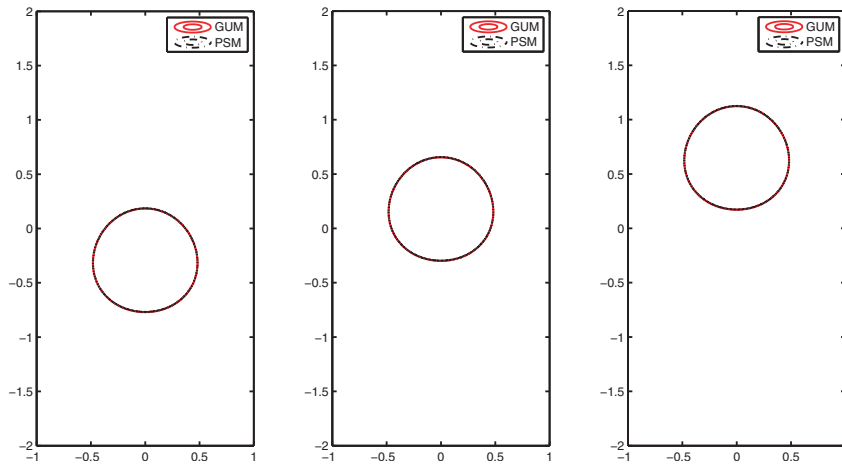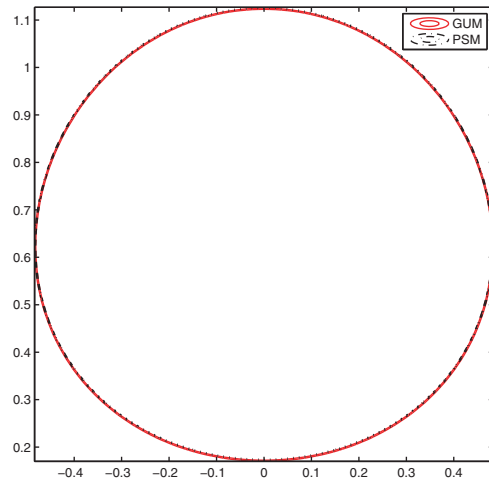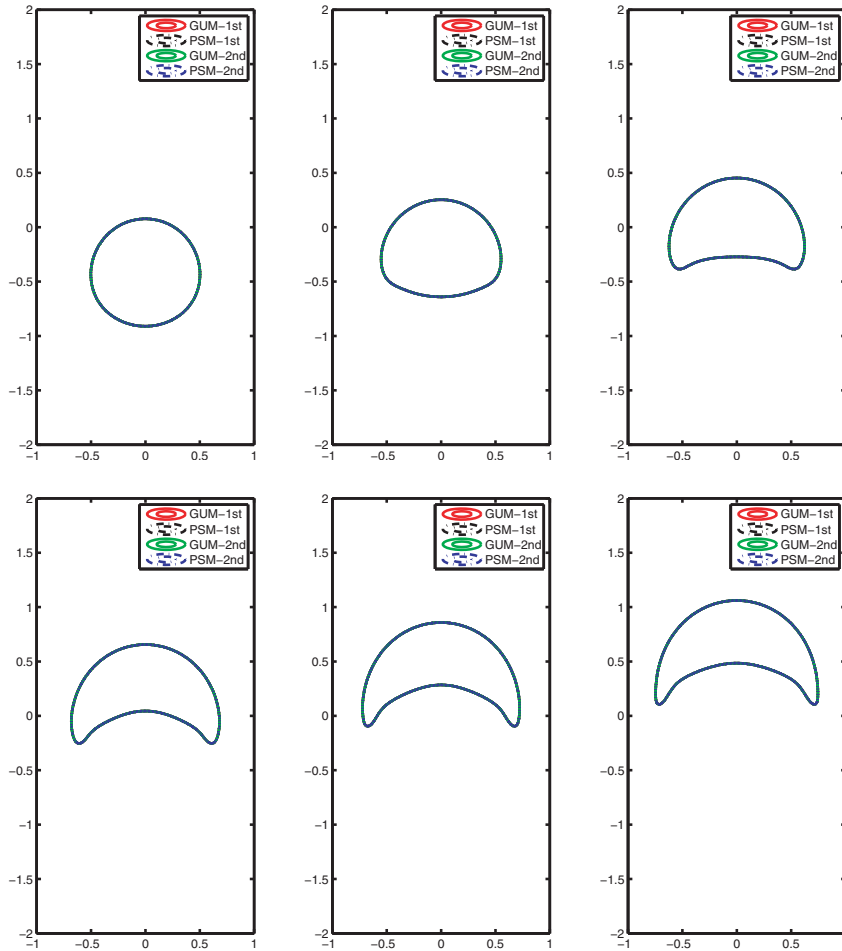
(a) Interfaces at different time snapshots $t = 2, 6, 10$.
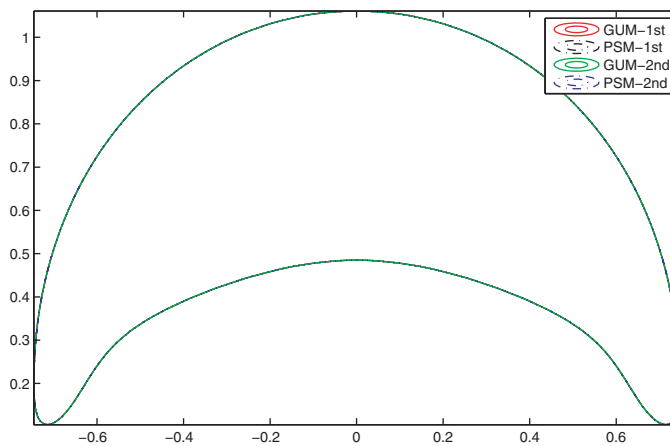

(b) Interface at $t = 10$.

FIG. 2. *Low density ratio with homogeneous viscosity, $\rho_1 = 1$ and $\rho_2 = 10$; comparisons of first-order PSM and GUM.*

5. Concluding remarks. We considered the modeling and numerical approximation of two-phase incompressible flows with different densities in this paper. The main contributions of the paper are as follows:

- We developed a physically consistent phase-field model for two-phase incompressible flows with different densities that admits an energy law.
- We constructed several efficient and energy stable time discretization schemes for the coupled nonlinear phase-field system. At each time step, these schemes all reduce to a weakly coupled system for the velocity and phase function and an elliptic or Poisson equation for the pressure. In particular, the schemes based on pressure stabilization only require solving a pressure Poisson equation. Thus, they are particularly efficient for problems with large density ratios.

(a) Interfaces at different time snapshots $t = 0.5, 1, 1.5, 2, 2.5, 3$.

(b) Interface at $t = 3$.

FIG. 3. *Air bubble in water,* $\rho_1 = 1.161$, $\rho_2 = 995.65$, $\mu_1 = 0.0000186$, *and* $\mu_2 = 0.0007977$ *at times snapshots* $t = 0.5, 1, 1.5, 2, 2.5, 3$. *Interfacial contours by the first- and second-order PSM and GUM.*

- Despite the decoupling of the pressure from the velocity and the very weak coupling between the velocity and the phase function, we were still able to prove that these schemes admit energy laws which are discrete counterparts of the continuous energy law.
- We carried out ample numerical experiments to compare the accuracy and efficiency of the four proposed schemes, and we performed challenging simulations of an air bubble rising in water.

While we have only considered the phase-field model based on the Allen–Cahn phase equation, it is clear that similar schemes can be constructed for the phase-field model based on the Cahn–Hilliard phase equation. It is expected that the stability proofs in section 3 can be directly extended to the Cahn–Hilliard case, but their numerical implementation will involve solving fourth-order equations.

REFERENCES

[1] D. M. Anderson, G. B. McFadden, and A. A. Wheeler, *Diffuse-interface methods in fluid mechanics*, Annu. Rev. Fluid Mech., 30 (1998), pp. 139–165.
[2] R. Becker, X. Feng, and A. Prohl, *Finite element approximations of the Ericksen–Leslie model for nematic liquid crystal flow*, SIAM J. Numer. Anal., 46 (2008), pp. 1704–1731.
[3] A. J. Chorin, *Numerical solution of the Navier-Stokes equations*, Math. Comp., 22 (1968), pp. 745–762.
[4] H. Ding, P. D. M. Spelt, and C. Shu, *Calculation of two-phase Navier-Stokes flows using phase-field modeling*, J. Comput. Phys., 226 (2007), pp. 2078–2095.
[5] W. E and J.-G. Liu, *Gauge method for viscous incompressible flows*, Commun. Math. Sci., 1 (2003), pp. 317–332.
[6] X. Feng, Y. He, and C. Liu, *Analysis of finite element approximations of a phase field model for two-phase fluids*, Math. Comp., 76 (2007), pp. 539–571.
[7] J.-L. Guermond and L. Quartapelle, *A projection FEM for variable density incompressible flows*, J. Comput. Phys., 165 (2000), pp. 167–188.
[8] J.-L. Guermond and A. Salgado, *A splitting method for incompressible flows with variable density based on a pressure Poisson equation*, J. Comput. Phys., 228 (2009), pp. 2834–2846.
[9] J. L. Guermond, P. Minev, and J. Shen, *An overview of projection methods for incompressible flows*, Comput. Methods Appl. Mech. Engrg., 195 (2006), pp. 6011–6045.
[10] M. E. Gurtin, D. Polignone, and J. Viñals, *Two-phase binary fluids and immiscible fluids described by an order parameter*, Math. Models Methods Appl. Sci., 6 (1996), pp. 815–831.
[11] D. Jacqmin, *Diffuse interface model for incompressible two-phase flows with large density ratios*, J. Comput. Phys., 155 (2007), pp. 96–127.
[12] P. Lin, C. Liu, and H. Zhang, *An energy law preserving C^0 finite element scheme for simulating the kinematic effects in liquid crystal dynamics*, J. Comput. Phys., 227 (2007), pp. 1411–1427.
[13] C. Liu and J. Shen, *A phase field model for the mixture of two incompressible fluids and its approximation by a Fourier-spectral method*, Phys. D, 179 (2003), pp. 211–228.
[14] C. Liu and N. J. Walkington, *Convergence of numerical approximations of the incompressible Navier–Stokes equations with variable density and viscosity*, SIAM J. Numer. Anal., 45 (2007), pp. 1287–1304.
[15] J. Lowengrub and L. Truskinovsky, *Quasi-incompressible Cahn-Hilliard fluids and topological transitions*, Philos. Trans. R. Soc. Lond. Ser. A Math. Phys. Eng. Sci., 454 (1998), pp. 2617–2654.
[16] R. Nochetto and J.-H. Pyo, *The gauge-Uzawa finite element method. Part I: The Navier–Stokes equations*, SIAM J. Numer. Anal., 43 (2005), pp. 1043–1068.
[17] S. Popinet, *An accurate adaptive solver for surface-tension-driven interfacial flows*, J. Comput. Phys., 228 (2009), pp. 5838–5866.
[18] A. Prohl, *Projection and Quasi-Compressibility Methods for Solving the Incompressible Navier-Stokes equations*, Adv. in Numer. Math., B. G. Teubner, Stuttgart, 1997.
[19] J. Pyo and J. Shen, *Gauge-Uzawa methods for incompressible flows with variable density*, J. Comput. Phys., 221 (2007), pp. 181–197.
[20] R. Rannacher, *On Chorin's projection method for the incompressible Navier-Stokes equations*, Lecture Notes in Math. 1530, 1991.
[21] L. Rayleigh, *On the theory of surface forces* ii, Phil. Mag., 33 (1892), p. 209.

[22] J. SHEN AND X. YANG, *An efficient moving mesh spectral method for the phase-field model of two-phase flows*, J. Comput. Phys., 228 (2009), pp. 2978–2992.

[23] J. SHEN, *On error estimates of the projection methods for the Navier–Stokes equations: First-order schemes*, SIAM J. Numer. Anal., 29 (1992), pp. 57–77.

[24] J. SHEN, *Efficient spectral-Galerkin method* I. *Direct solvers for second- and fourth-order equations by using Legendre polynomials*, SIAM J. Sci. Comput., 15 (1994), pp. 1489–1505.

[25] J. SHEN, *On error estimates of projection methods for the Navier-Stokes equations: Second-order schemes*, Math. Comp., 65 (1996), pp. 1039–1065.

[26] R. TEMAM, *Sur l'approximation de la solution des équations de Navier-Stokes par la méthode des pas fractionnaires* ii, Arch. Ration. Mech. Anal., 33 (1969), pp. 377–385.

[27] J. VAN DER WAALS, *The thermodynamic theory of capillarity under the hypothesis of a continuous density variation*, J. Stat. Phys., 20 (1893), pp. 197–244.

[28] X. YANG, J. J. FENG, C. LIU, AND J. SHEN, *Numerical simulations of jet pinching-off and drop formation using an energetic variational phase-field method*, J. Comput. Phys., 218 (2006), pp. 417–428.

[29] P. YUE, J. J. FENG, C. LIU, AND J. SHEN, *A diffuse-interface method for simulating two-phase flows of complex fluids*, J. Fluid Mech., 515 (2004), pp. 293–317.